

Experimental and theoretical studies of H₂O oxidation by neutral Ti₂O_{4,5} clusters under visible light irradiation†

Cite this: *Phys. Chem. Chem. Phys.*, 2014, 16, 13900

Shi Yin and Elliot R. Bernstein*

A new photo excitation fast flow reactor system is constructed and used to investigate reactions of neutral Ti_mO_n clusters with H₂O under visible (532 nm) light irradiation. Single photon ionization at 118 nm (10.5 eV) is used to detect neutral cluster distributions through time of flight mass spectrometry. Ti_mO_n clusters are generated through laser ablation of a titanium target in the presence of 4% O₂/He carrier gas. Association products Ti₂O₄(H₂O) and Ti₂O₅(H₂O) are observed for reactions of H₂O and Ti_mO_n clusters without irradiation. Under 532 nm visible light irradiation of the fast flow reactor, only the Ti₂O₅(H₂O) feature disappears. This light activated reaction suggests that visible radiation can induce chemistry for Ti₂O₅(H₂O), but not for Ti₂O₄(H₂O). Density functional theory (DFT) and time-dependent (TD) DFT calculations are performed to explore the ground and first excited state potential energy surfaces (PES) for the reaction Ti₂O₅ + H₂O → Ti₂O₄ + H₂O₂. A high barrier (1.33 eV) and a thermodynamically unfavorable (1.14 eV) pathway are obtained on the ground state PES for the Ti₂O₅ + H₂O reaction; the reaction is also thermodynamically unfavorable (1.54 eV) on the first singlet excited state PES. The reaction is proposed to occur on the ground state PES through a conical intersection (S₁/S₀)_{CI}, and to generate products Ti₂O₄ and H₂O₂ on the ground state PES. This mechanism is substantiated by a multi-reference *ab initio* calculation at the complete active space self-consistent field (CASSCF) level. The S₀–S₁ vertical excitation energy of Ti₂O₄ (3.66 eV) is much higher than the 532 nm photon energy (2.33 eV), suggesting this visible light driven reaction is unfavorable for the Ti₂O₄ cluster. The TDDFT calculated optical absorption spectra of Ti₂O₄ and Ti₂O₅ further indicate that Ti₂O₅ like structures on a titanium oxide surface are the active catalytic sites for visible light photo-catalytic oxidation of water.

Received 8th January 2014,
Accepted 27th May 2014

DOI: 10.1039/c4cp00097h

www.rsc.org/pccp

Introduction

Titanium oxide has attracted particular interest in recent years due to its potential application as a photo-catalyst. Photo-catalysis on the surface of titanium oxide is one of the most promising technologies for converting solar energy into chemical energy.^{1–5} Titanium oxide is also a good medium for environmental cleanup through activation of the photo-oxidation of organic pollutants on self-cleaning surfaces.⁶ The effect of hydrogen peroxide (H₂O₂) on the TiO₂ photo-catalytic activity under UV light irradiation has recently been studied. This research has been focused on enhancing the efficiency of organic pollutant removal in the

presence of H₂O₂.^{7,8} Some studies on the formation of H₂O₂ in an aqueous TiO₂ dispersion under UV irradiation have also been reported:^{9,10} several mechanisms have been proposed to explain hydrogen peroxide formation.

Hydrogen peroxide is a clean oxidant that emits only water as a byproduct and is widely used in industry for organic synthesis, pulp bleaching, wastewater treatment, and disinfection with high atom efficiency.^{11,12} At present, H₂O₂ is commercially produced by the anthraquinone method, but the process has some non-green features, such as high energy utilization because of multistep hydrogenation and oxidation reactions, so photocatalytic H₂O₂ synthesis with titanium dioxide has attracted much attention.^{13–15} The reaction is usually carried out by UV irradiation of oxygen saturated water with catalyst in the presence of an electron donor (*e.g.*, alcohols). The reaction proceeds at room temperature without evolution of H₂ gas and can be a clean and safe H₂O₂ synthesis.

Atomic/molecular level mechanisms for condensed phase catalytic reactions are suggested to be accurately modeled and understood through the study of gas phase cluster reactions.^{16–19}

Department of Chemistry, NSF ERC for Extreme Ultraviolet Science and Technology, Colorado State University, Fort Collins, CO 80523, USA.
E-mail: erb@lamar.colostate.edu

† Electronic supplementary information (ESI) available: Cartesian coordinates for optimized geometries (Å), total energies at 0 K (E_{0K}, a.u.), and zero point correction energies (ZPCE, a.u.) of intermediates and transition states at B3LYP/TZVP level, in Fig. 3 and 7 are given in Tables S1 and S2, respectively. See DOI: 10.1039/c4cp00097h

Titanium oxide clusters have thereby been the subject of intense investigation in recent years, and evolving cluster models have been frequently employed in theoretical calculations of titanium dioxide bulk or surface properties,^{20–22} even though the physical and chemical properties of TiO_2 nanomaterials, namely nanowires, nanoparticles and clusters, might be different from those of bulk titania.²³ In general, the ratio of surface to volume atoms increases as the cluster size decreases; accordingly, smaller TiO_2 nanoparticles have more active sites, with respect to photo-catalytic applications, because of the high density of surface corner, step, and edge atoms. Such as, the catalytic activity of TiO_2 materials is enhanced as the size and the dimension of these materials decrease.²⁴ Hence, titanium oxide atomic clusters have long been employed as models from which to gain fundamental insights into complicated surfaces and catalysts: small titanium oxide clusters might exhibit interesting quantum size effects and can be the starting points for understanding photo-catalytic processes.

Numerous experimental^{25–32} and theoretical^{33–42} studies have been reported for isolated, neutral and charged titanium oxide clusters with the intent of correlating their structures and properties with those of the bulk. For example, Zhai *et al.*²⁵ have studied the electronic structure and band gap evolution of $(\text{TiO}_2)_n^-$ ($n = 1–10$) clusters, employing photoelectron spectroscopy, to gain mechanistic understanding of TiO_2 surface defects and photo-catalytic properties. Their neutral cluster distribution has been reported by Matsuda *et al.*²⁶ for both unsaturated and saturated oxygen growth conditions, through 118 nm single photon ionization. $(\text{TiO}_2)_n$ anatase-like clusters with varying n values between 16 and 32 have been constructed theoretically,³⁶ and a general rule has been extracted stating that proper nano crystals are stoichiometric clusters that have a balanced charge distribution, with all constituent atoms having sufficiently high coordination to support their formal oxidation state. Infrared photodissociation spectroscopy and density functional theory (DFT) calculations of the interaction of TiO^+ with water, demonstrate that a $\text{Ti}(\text{OH})_2^+$ type product is dominant for this process.⁴² The structure of neutral $(\text{TiO}_2)_n$ ($n = 2–13$) clusters⁴³ and reliable values for the heats of formation of small $(\text{TiO}_2)_n$ ($n = 1–3$) clusters⁴⁴ have been reported. These structures and energies can be useful for understanding the general chemistry of $(\text{TiO}_2)_n$ species. The hydrolysis reactions of small TiO_2 clusters⁴⁵ and H_2 and O_2 production from water splitting by small TiO_2 clusters⁴⁶ have been studied theoretically, as well. Water readily reacts with both singlet and triplet states of $(\text{TiO}_2)_n$ ($n = 1–4$) clusters to form hydroxides, because reaction barriers are less than the H_2O complexation energies: the water splitting reaction has a lower barrier on the triplet state potential energy surface.

A number of experimental and theoretical studies have appeared on neutral and negatively and positively charged titanium oxide clusters, but to the best of our knowledge, the visible photo-catalytic oxidation of water by gas phase neutral titanium oxide species has not been reported. In this paper, we present the first study of visible photo-catalytic oxidation of water over neutral Ti_2O_5 clusters at room temperature. We employ a newly constructed

photo-excitation fast flow reactor system coupled with single photon ionization (SPI), which has proved to be reliable for detecting the distribution and reactivity of neutral clusters without dissociation or fragmentation.^{26,47,48} To demonstrate this reaction, DFT, time-dependent (TD) DFT, and finally multi-configurational, complete active space self-consistent field (CASSCF) calculations are performed to investigate the activity of Ti_mO_n clusters toward water oxidation on the ground and first excited state potential energy surfaces (PES). The experimental results are well interpreted by the calculations. Active sites and details of the reaction mechanism are obtained: we propose related condensed phase, atomic/molecular level, catalytic processes for water oxidation by O_3 over titanium oxide under visible light irradiation.

Methods

A. Experimental procedures

The experimental setup for laser ablation employed in this work has been described previously in detail.^{49–52} A new photo-excitation fast flow reactor system is constructed in order to investigate reactions of neutral Ti_mO_n clusters with H_2O under visible light irradiation. A schematic picture of the photo-excitation fast flow reactor system is shown in Fig. 1. Ti_mO_n clusters are generated in a laser ablation source: titanium plasma, ablated from a titanium foil disk, reacts with oxygen seeded in helium (4% O_2/He) expansion gas. One 10 Hz, focused, 532 nm $\text{Nd}^{3+}\text{:YAG}$ laser ($\text{Nd}^{3+}\text{:yttrium aluminum garnet}$) with ~6 mJ per pulse energy is used for the laser ablation. The other 10 Hz, defocused, 532 nm $\text{Nd}^{3+}\text{:YAG}$ laser with ~25 mJ per pulse energy is used for the laser light irradiation dispersed over the quartz reactor. The expansion gas is pulsed into the vacuum by a supersonic nozzle (R. M. Jordan, Co.) with a backing pressure of typically 75 psi. Synthesized Ti_mO_n clusters react with reactants in a fast flow quartz reactor (i.d. 6.8 mm × 68 mm), which is directly coupled to the cluster generation channel (i.d. 1.8 mm × 19 mm), with or without the 532 nm laser light irradiation. The reactant gas (H_2O), carried by helium (10 psi backing pressure,

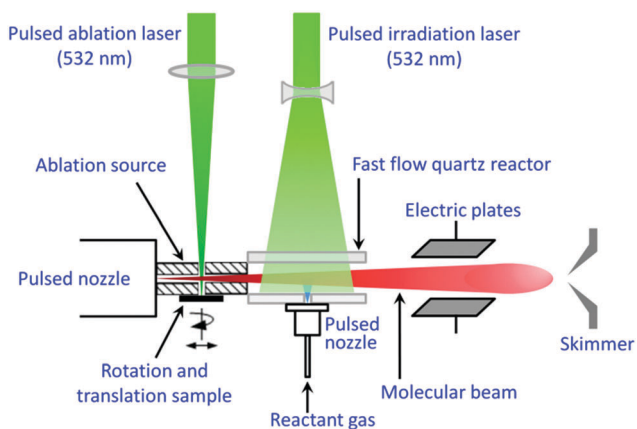


Fig. 1 A schematic figure of experimental setup with a photo-excitation fast flow reactor system.

bubbled through distilled water), is injected into the reactor flow tube by a pulsed General Valve (Parker, Series 9). The timing between the Jordan valve and the General Valve openings is optimized for the best product yields, and the timing between the General Valve opening and light irradiation laser firing is optimized for the best light irradiation reaction results.

The pressure in the fast flow reactor can be estimated ~ 14 Torr for the reaction.⁵³ Reactants and products are thermalized to 300–400 K by collision during the reaction.⁵⁴ An electric field is placed downstream of the reactor in order to remove any residual ions from the molecular beam. The beam of neutral reactants and products is skimmed into a differentially pumped chamber and ionized by a separated VUV laser beam (118 nm, 10.5 eV per photon). The 118 nm laser light is generated by focusing the third harmonic (355 nm, ~ 30 mJ) of a Nd³⁺:YAG laser in a tripling cell that contains about a 250 Torr argon/xenon (10/1) gas mixture. An MgF₂ prism (Crystaltechno LTD, Russia, 6° apex angle) is placed into the laser beam to enhance separation of the generated 118 nm laser beam from the 355 nm input laser beam. After the near threshold ionization, photoions are detected by a time of flight mass spectrometer (TOFMS).

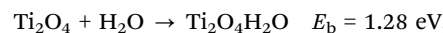
B. Calculational procedures

Calculations of the structural parameters for neutral Ti_{*m*}O_{*n*} clusters and the reactions of H₂O, N₂O, NO₂ and O₃ with Ti₂O_{4,5} clusters are performed employing density functional theory. The hybrid B3LYP exchange–correlation functional^{55–57} and a triple- ζ valence plus polarization (TZVP) basis set⁵⁸ are used. This choice of the B3LYP/TZVP method with moderate computational cost has been tested to provide reasonable results in previous studies on reactivity of titanium oxide clusters;⁵⁹ the approach yields good results for the assignment of infrared multi-photon dissociation spectra of titanium oxide clusters.⁶⁰ Binding energies between neutral Ti_{*m*}O_{*n*} and reactants are calculated at different typical association geometries to obtain the lowest energy structures. DFT and TDDFT calculations are performed to explore the ground and first excited state PES for the reaction Ti₂O₅ + H₂O → Ti₂O₄ + H₂O₂, involving geometry optimizations of the reactants, intermediates, transition states, and products. The geometry at conical intersections is optimized with state averaging over the S₀ and S₁ states with equal weights at the complete active space multiconfiguration self-consistent field (CASSCF) level of theory employing a 6-31g(d) basis set.⁶¹ Vibrational frequency calculations are further performed to confirm the global minima and transition states, which have zero and one imaginary frequency, respectively. The relative energies (given in eV) are corrected for zero point energy (ZPE) contributions. Additionally, intrinsic reaction coordinate (IRC) calculations are carried out to determine that an estimated transition state connects two appropriate local minima along the reaction pathway. Binding energies are calculated for a few species employing the Basis Set Superposition Error (BSSE) counterpoise correction;^{62,63} these corrections are found to be insignificant at the present level of theory.

Results and discussion

Fig. 2(a) shows the distribution of neutral titanium oxide clusters within the mass range of *m/z* = 150–200 detected employing 118 nm SPI-TOFMS. The distribution, which is generated by laser ablation of a titanium foil disk with 4% O₂ seeded in helium carrier gas, is similar to that observed by different ionization methods reported previously.²⁶ The Ti_{*m*}O_{2*m*} and Ti_{*m*}O_{2*m*+1} series are found to be the most stable neutral cluster species for high oxygen content in the expansion gas.

Mass spectra generated from the reaction of small neutral titanium oxide (Ti₂O_{4,5}) clusters with H₂O are presented in Fig. 2(b). By way of comparison, Fig. 2(a) shows the TOFMS for Ti₂O_{4,5} cluster distribution passing through an empty reaction cell. Associated products Ti₂O₄H₂O and Ti₂O₅H₂O are observed when H₂O is used as a reactant, indicating both neutral Ti₂O₄ and Ti₂O₅ clusters are able to adsorb single water molecules, and form stable association products. The calculation results suggest the binding energies (*E*_b) of Ti₂O₄ and Ti₂O₅ clusters with H₂O are close and around ~ 1.30 eV. These calculation results are in agreement with a theoretical study of the interactions of neutral (TiO₂)_{*n*} (*n* = 1–9) clusters with water,³⁷ which suggests a single water molecule binds to each cluster resulting in an average binding energy of ~ 1.1 eV. The Ti₂O_{4,5}–H₂O binding energies are:



The signal intensity of Ti₂O₅(H₂O) decreases a lot (from 0.5 to 0.2 eV, comparing Fig. 2(b) with Fig. 2(c)) when 532 nm laser light irradiates the fast flow quartz reactor, while the Ti₂O₄(H₂O) feature remains unchanged (Fig. 2(c)). The signal

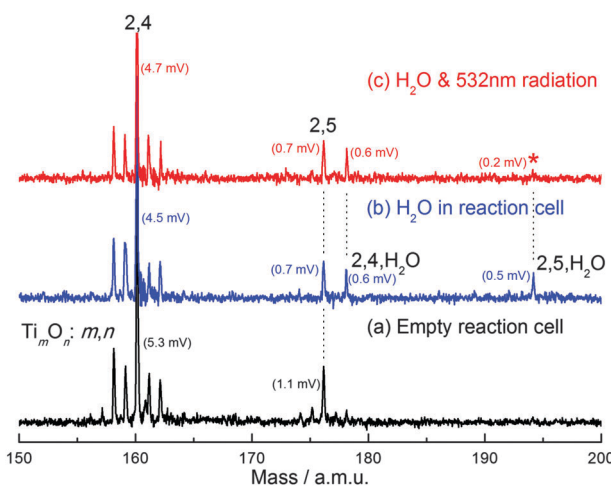


Fig. 2 Reactions of neutral Ti₂O_{4,5} clusters with H₂O with and without 532 nm light irradiation: (a) empty reaction cell, (b) H₂O vapor in reaction cell, and (c) H₂O vapor in reaction cell with 532 nm radiation. Products are labeled as Ti_{*m*}O_{*n*}(H₂O)_{0,1}: *m*, *n*. The signal intensity of all clusters given in mV is from average of three measurements at the same experimental condition. The asterisk in (c) marks the position of the decreased mass peak of Ti₂O₅H₂O. See text for details.

intensity of Ti_2O_5 does not change and the increase of Ti_2O_4 (~ 0.2 mV) is observed in Fig. 2(c) (compared with that in Fig. 2(b)). These observations suggest the likely reaction, $\text{Ti}_2\text{O}_5 + \text{H}_2\text{O} + h\nu_{(532\text{nm})} \rightarrow \text{Ti}_2\text{O}_4 + \text{H}_2\text{O}_2$.

The potential energy surface of ground (S_0) and first singlet excited states (S_1) for the reaction $\text{Ti}_2\text{O}_5 + \text{H}_2\text{O} \rightarrow \text{Ti}_2\text{O}_4 + \text{H}_2\text{O}_2$ are studied at the B3LYP/TZVP level by DFT and TDDFT calculation (Fig. 3), respectively. The Ti_2O_5 cluster contains two bridge-bonded (O_b) and three terminally bonded (O_t) oxygen atoms, and two titanium atoms: Ti_{I} , which bonds with one O_b , and Ti_{II} , which bonds with two O_t . On the S_0 potential energy surface (PES, shown in Fig. 3, dashed black line), the reaction starts with an exothermic addition of H_2O to Ti_{I} of singlet Ti_2O_5 to form a stable complex, $\text{Ti}_2\text{O}_5(\text{H}_2\text{O})$ (intermediate **G1**), with 1.34 eV adsorption energy, which is similar to the reported Lewis acid-base donor-acceptor bond formation during water adsorption on $(\text{TiO}_2)_{1,2}$ clusters.⁴⁵ An H atom transfers from H_2O to an O_t atom on Ti_{II} (through transition state **G2/G3**), leading to the formation of two -OH moieties on the Ti_{II} atom (intermediate **G3**). The reaction barrier from intermediate **G2** to **G3** is calculated to be only 0.3 eV. Then the S_0 PES possesses a significant, high overall reaction

barrier (ORB) for the reaction of 1.33 eV. This ORB is determined for the transformation of intermediate **G3** to intermediate **G4** through transition state **G3/G4**, during which step the H_2O_2 moiety attached to a Ti atom of Ti_2O_4 is formed (**G4**). The evaporation of the H_2O_2 moiety from **G5** leads to the formation of products $\text{Ti}_2\text{O}_4 + \text{H}_2\text{O}_2$ (**P1**), whose energy is 1.14 eV higher than that of the reactants $\text{Ti}_2\text{O}_5 + \text{H}_2\text{O}$ of the entrance of channel. Both the positive high ORB (1.33 eV) and the thermodynamic unavailable (1.14 eV) results indicate that the reaction ($\text{Ti}_2\text{O}_5 + \text{H}_2\text{O} \rightarrow \text{Ti}_2\text{O}_4 + \text{H}_2\text{O}_2$) cannot occur on the ground state PES at room temperature. This calculational result is in good agreement with the experimental observation presented in Fig. 2(b), in which a stable associated product $\text{Ti}_2\text{O}_5\text{H}_2\text{O}$ is observed.

The S_0 - S_1 vertical excitation energy of Ti_2O_5 (2.48 eV, calculated by TDDFT) is close to the 532 nm photon energy (2.33 eV), which suggests the ground state Ti_2O_5 can absorb a 532 nm photon and be excited to its first singlet excited state. On the first excited state (S_1) PES, the reaction is also found to be thermodynamically unfavorable (1.54 eV) for generation of excited state products **P2**, as shown in Fig. 3 (dashed blue line).

The observed reaction of excited state Ti_2O_5^* with H_2O is thereby suggested to occur through a conical intersection ($(S_1/S_0)_{\text{CI}}$), with generation of products Ti_2O_4 and H_2O_2 on the ground state PES, following the reaction path shown in Fig. 3 (red line). A water molecule preferentially binds to the Ti_{I} atom of the excited Ti_2O_5^* cluster through its oxygen atom with no barrier to form a stable intermediate **E1**, which is 1.88 eV lower in energy than the reactants ($\text{Ti}_2\text{O}_5^* + \text{H}_2\text{O}$). Next, the H_2O transfers to the Ti_{II} site through transition state **E1/E2**, and the HO-H bond ruptures through transition state **E2/E3** to generate the $\text{Ti}_2\text{O}_4(\text{OH})_2^*$ complex (intermediate **E3**) in barrierless processes. Intermediate **E3** descends to the ground state through conical intersection ($S_1/S_0)_{\text{CI}}$ and then generates intermediate **G4**, which contains a formed $-\text{H}_2\text{O}_2$ moiety binding to a Ti atom of Ti_2O_4 , via transition state **G3/G4**, now all on the S_0 PES. The ground state products Ti_2O_4 and H_2O_2 (**P1**) are finally generated barrierlessly and thermodynamically favorably from the reaction of Ti_2O_5^* (absorbing a 532 nm photon) with H_2O . Note that the conical intersection between the ground state and first excited state is searched at the CASSCF(10,7)/6-31G(d) level. Geometry of the conical intersection is optimized with state averaging over the S_0 and S_1 states with equal weight. Orbitals chosen for the active space, illustrated in Fig. 4, are mostly located on the two -OH moieties and the terminal oxygen bonding with the same Ti atom. These selected sites of the clusters are important for the formation of the $-\text{H}_2\text{O}_2$ moiety (from intermediate **E3** to intermediate **G4** via transition state **G3/G4**). The adiabatic energy gap between S_0 and S_1 for this conical intersection is 0.002 eV. The small adiabatic energy gap between S_0 and S_1 suggests that the S_1 and S_0 surfaces are strongly coupled at this conical intersection point. This strong coupling implies that the reaction occurs through transition from the excited state to the ground state through this conical intersection ($S_1/S_0)_{\text{CI}}$. In a reaction force ($-\Delta E/\Delta A$) calculation, in which E is the potential energy and A is the angle along the reaction coordinate ($\langle \text{HO-Ti-O}, S_0, \text{G3} \rangle$ and $\langle \text{HO-Ti-OH}, S_0, \text{G4} \rangle$,

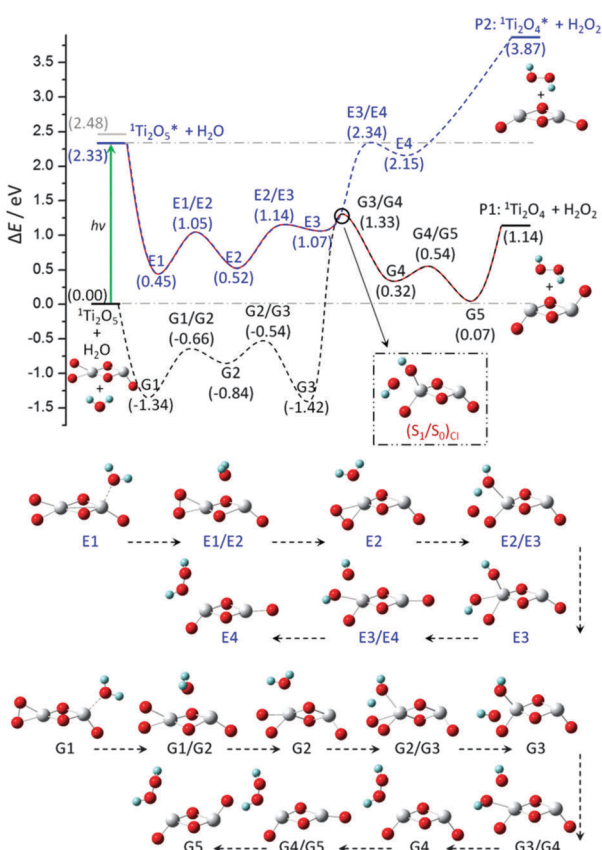


Fig. 3 A potential energy surface profile of ground and first singlet excited states for the reaction $\text{Ti}_2\text{O}_5 + \text{H}_2\text{O} \rightarrow \text{Ti}_2\text{O}_4 + \text{H}_2\text{O}_2$. Energies are in eV, relative to the initial reactant energy of ${}^1\text{Ti}_2\text{O}_5 + \text{H}_2\text{O}$. Energy levels are calculated at the B3LYP/TZVP theory level. The spin multiplicity (M) is listed as ${}^M\text{Ti}_2\text{O}_{4,5}$. “ $(S_1/S_0)_{\text{CI}}$ ” denotes a conical intersection for the ground and excited state potential energy surfaces. Geometry of the $(S_1/S_0)_{\text{CI}}$ is calculated at the CASSCF(10,7)/6-31g(d) level. See text for details.

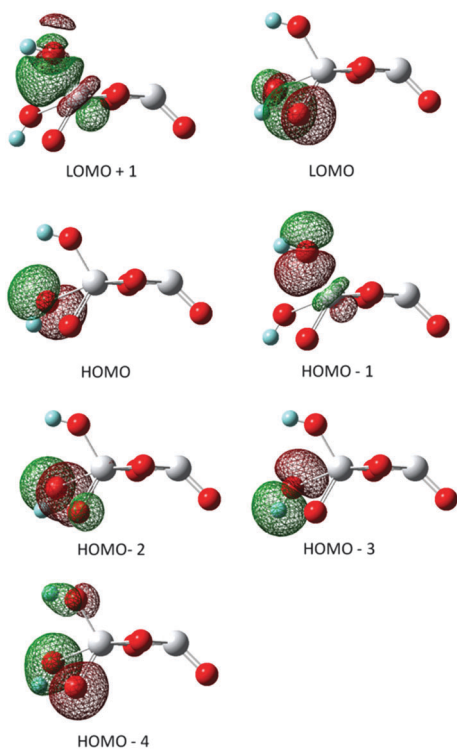


Fig. 4 Orbitals used in the active space (10,7) for CASSCF calculations for the conical intersection (S_1/S_0)_{CI}.

the absolute force for both reaction coordinate, $S_{0,G3}$ and $S_{0,G4}$ are similar, which suggests these two pathways (connecting with **G3** and **G4** from (S_1/S_0) _{CI}) are comparable. The formation of ground state products **P1** (Ti_2O_4 and H_2O_2) through (S_1/S_0) _{CI} is energetically acceptable and the potential energy of the molecule changes smoothly without any barriers (Fig. 3). Similar calculation results are also obtained at CASSCF(10,7)/6-31++g(d,p) level. Given that the reaction is actually observed to occur, this photon driven, S_1 to S_0 transition through (S_1/S_0) _{CI} appears to be a possible thermodynamically and kinetically available mechanism.

The S_0 to first triplet excited state (T_1) vertical excitation energy of Ti_2O_5 is 2.40 eV calculated by TDDFT (close to the 532 nm photon energy, 2.33 eV), which suggests the ground state Ti_2O_5 can absorb a 532 nm photon and be excited to its first triplet excited state. Nonetheless, the reaction is also found to be thermodynamically unfavorable (2.21 eV higher than the energy of initial reactants $^3Ti_2O_5^*$ + H_2O) for generation of excited state products $^3Ti_2O_4^*$ + H_2O_2 on its T_1 PES, so the reaction of $^3Ti_2O_5^*$ with H_2O must necessarily occur through an existent conical intersection ((T_1/S_0) _{CI}) to generate ground state products Ti_2O_4 and H_2O_2 . This mechanism employs all the available energy for the system for the photon driven reaction.

As given by the calculational results discussed above, one possible reaction mechanism for the water oxidation by Ti_2O_5 under light irradiation is that the Ti_2O_5 cluster is excited by irradiation, and then oxidizes the water. Ti_I atoms of reactive $Ti_2O_5^*$ clusters (excited by 532 nm light) are the active sites for holding H_2O molecules during the H_2O oxidation reaction process, and the terminal oxygen atoms on Ti_{II} are the active

oxygen for adsorbed H_2O oxidation reaction. Ground state products Ti_2O_4 and H_2O_2 can be generated by the steepest descent pathway from the excited state through the conical intersection ((S_1/S_0) _{CI}) to the S_0 PES. The proposed mechanism for this photo-catalytic reaction suggests the interaction of the S_0 and S_1 states of $Ti_2O_5 + H_2O$ through a non-adiabatic, conical intersection driven process similar to those proposed and demonstrated for organic photochemical systems.⁶⁴ Additionally, the S_0-S_1 vertical excitation energy of $Ti_2O_5H_2O$ (intermediate **G1**) is calculated to be 2.57 eV by TDDFT (also close to the 532 nm photon energy, 2.33 eV), which suggests the ground state association product $Ti_2O_5H_2O$ is also able to absorb a 532 nm photon and be excited to its first excited state; thereby, another possible reaction mechanism for the water oxidation by Ti_2O_5 under light irradiation can be proposed to be that the Ti_2O_5 cluster adsorbs a water molecule, and then the association product $Ti_2O_5H_2O$ is excited by 532 nm irradiation. Considering the reaction system temperature at 300–400 K, the excited $Ti_2O_5H_2O^*$ will have about 0.5 eV of vibrational energy. The ~2.83 eV (0.5 eV vibrational energy + 2.33 eV, adsorbed photon energy) excess energy in the excited $Ti_2O_5H_2O^*$ is enough to overcome reaction barriers, and to form ground state products Ti_2O_4 and H_2O_2 following the reaction path: excited $Ti_2O_5H_2O^*$ → intermediate **E1** → transition state **E1/E2** → intermediate **E2** → transition state **E2/E3** → intermediate **E3** → conical intersection (S_1/S_0)_{CI} → intermediate **G4** → transition state **G4/G5** → intermediate **G5** → ground state $Ti_2O_4 + H_2O_2$, as shown in Fig. 3. This potential reaction mechanism agrees with the experimental results: since the quantum efficiency of Ti_2O_5 excitation is not large (as shown the relative absorption cross section at 532 nm in Fig. 6), sufficient ground state Ti_2O_5 exists in the beam to yield ground state $Ti_2O_5(H_2O)$, but the mass signal of $Ti_2O_5(H_2O)$ decreases considerably upon light irradiation.

Other possible mechanisms (reaction coordinates) may exist for the reaction, $Ti_2O_5 + H_2O \rightarrow Ti_2O_4 + H_2O_2$, under visible light irradiation. Only two of them are discussed here. Of course as is typically observed for cluster formation in pick up cells, only some of the $Ti_{2,4,5}$ clusters interact with H_2O but all of the $Ti_2O_5(H_2O)$ react with light irradiation. Clearly, both Ti_2O_5 and formed $Ti_2O_5(H_2O)$ can absorb light and then react. The point here is not whether the light is absorbed before or after the water cluster is formed but that the conical intersection between the first excited and ground state potential energy surfaces is an essential component of the reaction coordinate and mechanism for either pathway, as it enables the absorbed energy to be part of the energy balance for the process. Some other potential reaction paths are also considered: for example, an H atom transfer from water to the O_tO_t moiety on Ti_{II} to form an $-OOH$ and then a subsequent H atom transfer from the remaining $-OH$ of water to the $-OOH$, (starting from intermediate **G2**, Fig. 3). Calculated energies for this path yield all ground transition states considerably lower than energies of the first singlet and triplet excited state intermediates along this reaction path. These energy differences do not support conical intersection between the ground state and first excited state potential energy surfaces for this reaction path,

and thereby, this path is not a viable reaction mechanism for our experimental results.

The experimental results presented in Fig. 2(c) demonstrate that the association product $\text{Ti}_2\text{O}_4(\text{H}_2\text{O})$ feature does not change under the visible light irradiation. The $S_0\text{-}S_1$ vertical excitation energy of Ti_2O_4 (3.66 eV), also calculated by TDDFT, is much higher than the 532 nm photon energy (2.33 eV): the Ti_2O_4 cluster does not absorb this 2.33 eV visible light. The reaction energy for $\text{Ti}_2\text{O}_4 + \text{H}_2\text{O} \rightarrow \text{Ti}_2\text{O}_3 + \text{H}_2\text{O}_2$ is also calculated to be 5.43 eV, thus the energy of a single photon (532 nm) is insufficient to overcome the endothermicity of this reaction.

The highest occupied molecular orbital (HOMO) and lowest unoccupied molecular orbital (LUMO) of neutral Ti_2O_4 and Ti_2O_5 clusters are presented in Fig. 5. The HOMO orbitals are dominated by the O-2p and the LUMO orbitals are dominated by the Ti-3d orbitals, which suggest the $S_0\text{-}S_1$ excitation of $\text{Ti}_{2,4,5}$ clusters are from O-2p to Ti-3d orbitals (ligand to metal charge transfer). The HOMO (O-2p) and LUMO (Ti-3d) character is also properly captured in the theoretical study of visible light absorption of the TiO_2 rutile structure.⁶⁵

In Fig. 6, we show the calculated optical absorption of Ti_2O_4 and Ti_2O_5 clusters using TDDFT calculations. The calculated absorption edge (solid black) for Ti_2O_4 cluster is ~ 400 nm (~ 3.0 eV) and is close to the experimental result (~ 2.9 eV) of optical absorbance spectrum for pure TiO_2 on a $\text{TiO}_2(110)$ surface.^{66,67} The lowest excitations are dominated by direct transitions from the O-2p states at the top of the valence band to the Ti-3d states at the bottom of the conduction band.⁶⁵ The Ti_2O_5 cluster spectrum (dashed red) has a main absorption at ~ 350 nm (~ 3.5 eV) and edge extending out to ~ 550 nm (~ 2.25 eV).

According to the calculated geometry, Ti_2O_4 has two bridging Ti-O single bonds (bond length 1.85 Å) and two terminal Ti=O double bonds (bond length 1.63 Å), and Ti_2O_5 have two bridging Ti-O single bonds (bond length between 1.84–1.87 Å), one terminal Ti=O double bond (bond length 1.62 Å), and two terminal Ti-O single bonds (bond length 1.82 and 1.84 Å). The lower absorption energy of Ti_2O_5 than that of Ti_2O_4 can be associated with its terminal Ti-O single bonded oxygen atoms, as the HOMO of Ti_2O_5 is composed mostly of the O_t-2p orbitals (Fig. 5). In other words, the single bond O_t-2p orbital composition

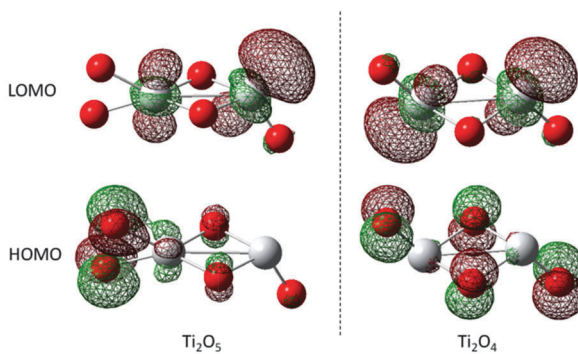


Fig. 5 DFT orbital plots showing the HOMO and LUMO of neutral $\text{Ti}_{2,4,5}$ clusters. The HOMOs are dominated by the O-2p and the LUMOs are dominated by the Ti-3d orbitals.

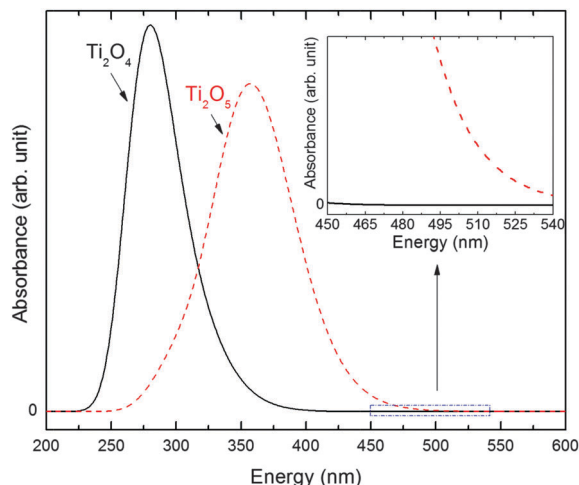
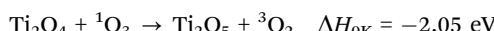
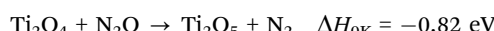
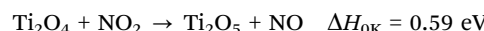


Fig. 6 Optical spectra of gas phase neutral Ti_2O_4 (black) and Ti_2O_5 (red) clusters using TDDFT calculations.

of the HOMO lowers the gap between the HOMO and LUMO of titanium oxide. These results suggest that the oxygen atoms of the terminal Ti-O single bonds on Ti_2O_5 are probably responsible for the observed calculated low absorption energy edge of this cluster (Fig. 6) and thereby its reactivity with H_2O under visible irradiation (Fig. 2(c)).

In the practical photo-catalytic oxidation of water by oxidants, the catalyst must be cycled. In order to generate a full catalytic cycle for water oxidation on titanium oxide clusters that can play an important role as catalysts, oxidation of Ti_2O_4 with different oxidants (NO_2 , N_2O , and O_3) is calculated to explore the potential regeneration of the photo-catalytically active titanium oxide cluster (Ti_2O_5) by different oxidants.



On the PES for the reaction of the Ti_2O_4 cluster with N_2O (Fig. 7), a high barrier (0.91 eV) is obtained for the reaction, although this reaction is thermodynamically favorable. Potential energy profiles for the oxidation of Ti_2O_4 by singlet and triplet O_3 (Fig. 7) are determined for O_3 attaching to the Ti sites on the Ti_2O_4 cluster. An overall reaction barrier (ORB) of 0.26 eV is determined for the reaction of Ti_2O_4 with singlet O_3 . For the reaction of Ti_2O_4 with triplet O_3 , the results in Fig. 7 shows that no ORB (or negative ORB of -1.81 eV, compared to the initial reactants ${}^1\text{Ti}_2\text{O}_4 + {}^1\text{O}_3$) exists for the oxidation of Ti_2O_4 . Note that the crossing of spin triplet and singlet potential energy surfaces (spin conversion⁶⁸) is obtained: this surface crossing suggests that the initial reactants ${}^1\text{Ti}_2\text{O}_4 + {}^1\text{O}_3$ can also form products ${}^1\text{Ti}_2\text{O}_5 + {}^3\text{O}_2$ through the spin conversion point (CP or CI) in Fig. 7. These calculation results suggest that ozone may be a good oxidant for regeneration of the visible photo catalytically reactive Ti_2O_5 clusters for water oxidation.

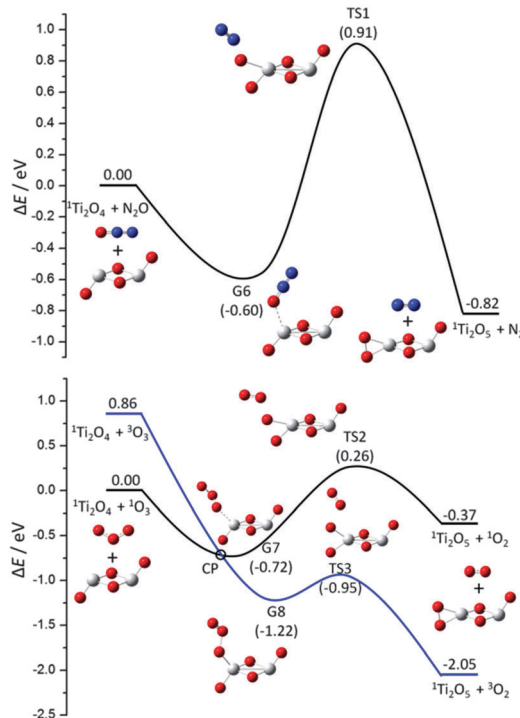


Fig. 7 Potential energy surface profiles of the ground state for reactions $\text{Ti}_2\text{O}_4 + \text{N}_2\text{O} \rightarrow \text{Ti}_2\text{O}_5 + \text{N}_2$ and $\text{Ti}_2\text{O}_4 + \text{O}_3 \rightarrow \text{Ti}_2\text{O}_5 + \text{O}_2$. Energies are in eV, relative to the initial reactant energy. Energy levels are calculated at the B3LYP/TZVP theory level. The spin multiplicity (M) is listed as ${}^1\text{Ti}_2\text{O}_{4,5}$, ${}^1\text{O}_2$, and ${}^3\text{O}_3$. "CP" denotes a possible spin conversion point for the O_3 singlet and triplet potential energy surfaces.

Reactive clusters in the gas phase can be seen as a good model system for the active moieties that exist on a catalyst surface. Thereby, a catalytic cycle for water oxidation by O_3 on titanium oxide surfaces can be proposed, and is presented in Fig. 8. This proposal is offered based on experimental and calculational results presented in Fig. 2, 3 and 7. Our proposed mechanism indicates that the H_2O molecule adsorbs on the Ti_{I} site, which binds to only one terminal oxygen atom, and reacts with the active O_{t} atom on the adjacent Ti_{II} site under visible light irradiation.

H_2O_2 molecules can be formed through O_{t} (on a Ti_{II} site) activation and desorbed leaving Ti_{I} sites on the catalytic

titanium oxide surface. O_3 molecules can then be adsorbed on the Ti_{I} sites through a terminal oxygen atom. The $\text{Ti}_{\text{II}}-\text{O}_{\text{t}}$ bonds are regenerated via O_2 molecules desorption, leaving the photo-catalytic titanium oxide surface unchanged. Water oxidation by O_3 is thereby possible over the titanium oxide catalyst surface under visible light irradiation. The catalytic cycle (schematically depicted in Fig. 8) is helpful to understand the heterogeneous visible photo-catalytic reaction mechanism of H_2O oxidation on the condensed phase catalyst surface. To enhance the visible photo-catalytic activity of a titanium oxide catalyst, one should try to increase the titanium sites with two terminal oxygen atoms at the surface.

Conclusions

A new photo excitation fast flow reactor system is constructed and used to investigate reactions of neutral Ti_mO_n clusters with H_2O under visible (532 nm) light irradiation. Association products $\text{Ti}_2\text{O}_4(\text{H}_2\text{O})$ and $\text{Ti}_2\text{O}_5(\text{H}_2\text{O})$ are observed for reactions of H_2O without irradiation. Under 532 nm light irradiation on the fast flow reactor, only the $\text{Ti}_2\text{O}_5(\text{H}_2\text{O})$ feature disappears. This light activated reaction suggests that visible (532 nm) radiation can induce chemistry for $\text{Ti}_2\text{O}_5(\text{H}_2\text{O})$, but not for $\text{Ti}_2\text{O}_4(\text{H}_2\text{O})$. DFT and TDDFT calculations are performed to explore the ground and first excited state PESs for the reactions $\text{Ti}_2\text{O}_5 + \text{H}_2\text{O} \rightarrow \text{Ti}_2\text{O}_4 + \text{H}_2\text{O}_2$. A high barrier (1.33 eV) and a thermodynamically unfavorable (1.14 eV) pathway are obtained on the ground state PES for the $\text{Ti}_2\text{O}_5 + \text{H}_2\text{O}$ reaction; the reaction is also thermodynamically unfavorable (1.54 eV) on the first excited state PES. Both the reaction of excited Ti_2O_5 (absorbing a 532 nm photon) with H_2O and the reaction of excited association product $\text{Ti}_2\text{O}_5\text{H}_2\text{O}$ (absorbing a 532 nm photon) are able to generate products Ti_2O_4 and H_2O_2 on the ground state PES through a conical intersection between the first excited and ground state potential energy surfaces. The conical intersection is an essential component of the reaction coordinate and mechanism for the water oxidation by Ti_2O_5 under light irradiation. Theoretical studies suggest that electronic excitation of $\text{Ti}_{2,4,5}$ clusters is from an $\text{O}-2\text{p}$ orbital (HOMO) to a $\text{Ti}-3\text{d}$ orbital (LUMO). The S_0-S_1 vertical excitation energy of Ti_2O_5 (2.48 eV) is smaller than that of Ti_2O_4 (3.66 eV), possibly because the Ti_2O_5 HOMO is composed mostly of 2p orbitals from single bonded terminal oxygens O_{t} , while the 2p orbitals for Ti_2O_4 comprising the HOMO are from the double bonded O_{t} and O_{b} atoms. The reaction mechanisms explored by calculations are in good agreement with the experimental results. The TDDFT calculated optical absorption spectra of Ti_2O_4 and Ti_2O_5 suggest that the Ti_2O_5 like structures on a titanium oxide surface are better active catalytic sites than Ti_2O_4 structures for visible light photo-catalysis of water oxidation.

Acknowledgements

This work is supported by a grant from the US Air Force Office of Scientific Research (AFOSR) through grant number

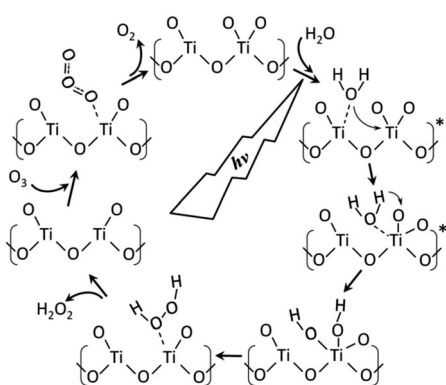


Fig. 8 Possible photo-catalytic cycle for water oxidation by O_3 over titanium oxide catalysts at the molecular level.

FA9550-10-1-0454, the National Science Foundation (NSF) ERC for Extreme Ultraviolet Science and Technology under NSF Award No. 0310717, and the National Science Foundation through XSEDE resources under grant number TG-CHE110083. We thank Dr Yan Xie for work on the construction of the photo excitation fast flow reactor system and Prof. S. G. He for original experiments on the $Ti_mO_n-H_2O-h\nu$ system.

Notes and references

- 1 T. Hirakawa and P. V. Kamat, *J. Am. Chem. Soc.*, 2005, **127**, 3928–3934.
- 2 T. L. Thompson and J. T. Yates, *Chem. Rev.*, 2006, **106**, 4428–4453.
- 3 S. Livraghi, M. C. Paganini, E. Giannello, A. Selloni, C. Di Valentin and G. Pacchioni, *J. Am. Chem. Soc.*, 2006, **128**, 15666–15671.
- 4 X. Chen and S. S. Mao, *Chem. Rev.*, 2007, **107**, 2891–2959.
- 5 S. U. M. Khan, M. Al-Shahry and W. B. Ingler, *Science*, 2002, **297**, 2243–2245.
- 6 S. Lacombe and N. Keller, *Environ. Sci. Pollut. Res.*, 2012, **19**, 3651–3654.
- 7 T. Y. Wei, Y. Y. Wang and C. C. Wan, *J. Photochem. Photobiol. A*, 1990, **55**, 115–126.
- 8 V. Auguliaro, E. Davi, L. Palmisano, M. Schiavello and A. Sclafani, *Appl. Catal.*, 1990, **65**, 101–116.
- 9 P. Salvador and F. Decker, *J. Phys. Chem.*, 1984, **88**, 6116–6120.
- 10 A. J. Hoffman, E. R. Carraway and M. R. Hoffmann, *Environ. Sci. Technol.*, 1994, **28**, 776–785.
- 11 J. M. Campos-Martin, G. Blanco-Brieva and J. L. G. Fierro, *Angew. Chem., Int. Ed.*, 2006, **45**, 6962–6984.
- 12 K. Sato, M. Aoki and R. Noyori, *Science*, 1998, **281**, 1646–1647.
- 13 S. Robl, M. Worner, D. Maier and A. M. Braun, *Photochem. Photobiol. Sci.*, 2012, **11**, 1041–1050.
- 14 Y. Shiraishi, S. Kanazawa, D. Tsukamoto, A. Shiro, Y. Sugano and T. Hirai, *ACS Catal.*, 2013, **3**, 2222–2227.
- 15 T. Hirakawa and Y. Nosaka, *J. Phys. Chem. C*, 2008, **112**, 15818–15823.
- 16 S. Yin and E. R. Bernstein, *Int. J. Mass Spectrom.*, 2012, **321**, 49–65.
- 17 M. Schlangen and H. Schwarz, *Catal. Lett.*, 2012, **142**, 1265–1278.
- 18 M. Y. Jia, B. Xu, X. L. Ding, S. G. He and M. F. Ge, *J. Phys. Chem. C*, 2012, **116**, 24184–24192.
- 19 X. Tang, X. Li, Y. Wang, K. Wepasnick, A. Lim, D. H. Fairbrother, K. H. Bowen, T. Mangler, S. Noessner, C. Wolke, M. Grossmann, A. Koop, G. Gantefoer, B. Kiran and A. K. Kandalam, *J. Phys.: Conf. Ser.*, 2013, **438**, 012005.
- 20 G. Pacchioni, A. M. Ferrari and P. S. Bagus, *Surf. Sci.*, 1996, **350**, 159–175.
- 21 C. Sousa and F. Illas, *Phys. Rev. B: Condens. Matter Mater. Phys.*, 1994, **50**, 13974–13980.
- 22 A. Hagfeldt, H. Siegbahn, S.-E. Lindquist and S. Lunell, *Int. J. Quantum Chem.*, 1992, **44**, 477–495.
- 23 D. Çakir and O. Gülsen, *Phys. Rev. B: Condens. Matter Mater. Phys.*, 2009, **80**, 125424.
- 24 M. Anpo, T. Shima, S. Kodama and Y. Kubokawa, *J. Phys. Chem.*, 1987, **91**, 4305–4310.
- 25 H. J. Zhai and L. S. Wang, *J. Am. Chem. Soc.*, 2007, **129**, 3022–3026.
- 26 Y. Matsuda and E. R. Bernstein, *J. Phys. Chem. A*, 2005, **109**, 314–319.
- 27 M. Foltin, G. J. Stueber and E. R. Bernstein, *J. Chem. Phys.*, 1999, **111**, 9577–9586.
- 28 H. Wu and L. S. Wang, *J. Chem. Phys.*, 1997, **107**, 8221–8228.
- 29 G. V. Chertihin and L. Andrews, *J. Phys. Chem.*, 1995, **99**, 6356–6366.
- 30 B. C. Guo, K. P. Kerns and A. W. Castleman Jr, *Int. J. Mass Spectrom. Ion Processes*, 1992, **117**, 129–144.
- 31 W. Yu and R. B. Freas, *J. Am. Chem. Soc.*, 1990, **112**, 7126–7133.
- 32 W. J. Zheng, J. M. Nilles, O. C. Thomas and K. H. Bowen, *Chem. Phys. Lett.*, 2005, **401**, 266–270.
- 33 Y. Z. Liu, Y. B. Yuan, Z. B. Wang, K. M. Deng, C. Y. Xiao and Q. X. Li, *J. Chem. Phys.*, 2009, **130**, 174308.
- 34 S. G. Li and D. A. Dixon, *J. Phys. Chem. A*, 2008, **112**, 6646–6666.
- 35 N. Marom, M. Kim and J. R. Chelikowsky, *Phys. Rev. Lett.*, 2012, **108**, 106801.
- 36 P. Persson, J. C. M. Gebhardt and S. Lunell, *J. Phys. Chem. B*, 2003, **107**, 3336–3339.
- 37 D. Çakir and O. Gülsen, *J. Phys.: Condens. Matter*, 2012, **24**, 305301.
- 38 O. A. Syzgantseva, P. Gonzalez-Navarrete, M. Calatayud, S. Bromley and C. Minot, *J. Phys. Chem. C*, 2011, **115**, 15890–15899.
- 39 L. Chiodo, M. Salazar, A. H. Romero, S. Laricchia, F. Della Sala and A. Rubio, *J. Chem. Phys.*, 2011, **135**, 244704.
- 40 F. Grein, *J. Chem. Phys.*, 2007, **126**, 034313.
- 41 Z. W. Qu and G. J. Kroes, *J. Phys. Chem. B*, 2006, **110**, 8998–9007.
- 42 H.-G. Xu, X.-N. Li, X.-Y. Kong, S.-G. He and W.-J. Zheng, *Phys. Chem. Chem. Phys.*, 2013, **15**, 17126–17133.
- 43 M. Chen and D. A. Dixon, *J. Chem. Theory Comput.*, 2013, **9**, 3189–3200.
- 44 S. Li, J. M. Hennigan, D. A. Dixon and K. A. Peterson, *J. Phys. Chem. A*, 2009, **113**, 7861–7877.
- 45 T.-H. Wang, Z. Fang, N. W. Gist, S. Li, D. A. Dixon and J. L. Gole, *J. Phys. Chem. C*, 2011, **115**, 9344–9360.
- 46 Z. Fang and D. A. Dixon, *J. Phys. Chem. A*, 2013, **117**, 3539–3555.
- 47 S. G. He, Y. Xie, Y. Q. Guo and E. R. Bernstein, *J. Chem. Phys.*, 2007, **126**, 194315.
- 48 Y. Matsuda, D. N. Shin and E. R. Bernstein, *J. Chem. Phys.*, 2004, **120**, 4142–4149.
- 49 S. Yin, Y. Xie and E. R. Bernstein, *J. Chem. Phys.*, 2012, **137**, 124304.
- 50 S. Yin, Y. Xie and E. R. Bernstein, *J. Phys. Chem. A*, 2011, **115**, 10266–10275.
- 51 S. G. He, Y. Xie, F. Dong, S. Heinbuch, E. Jakubikova, J. J. Rocca and E. R. Bernstein, *J. Phys. Chem. A*, 2008, **112**, 11067–11077.

- 52 S. Yin, Z. C. Wang and E. R. Bernstein, *Phys. Chem. Chem. Phys.*, 2013, **15**, 4699–4706.
- 53 W. Xue, Z. C. Wang, S. G. He, Y. Xie and E. R. Bernstein, *J. Am. Chem. Soc.*, 2008, **130**, 15879–15888.
- 54 M. E. Geusic, M. D. Morse, S. C. Obrien and R. E. Smalley, *Rev. Sci. Instrum.*, 1985, **56**, 2123–2130.
- 55 A. D. Becke, *Phys. Rev. A: At., Mol., Opt. Phys.*, 1988, **38**, 3098–3100.
- 56 A. D. Becke, *J. Chem. Phys.*, 1993, **98**, 5648–5652.
- 57 C. T. Lee, W. T. Yang and R. G. Parr, *Phys. Rev. B: Condens. Matter Mater. Phys.*, 1988, **37**, 785–789.
- 58 F. Weigend and R. Ahlrichs, *Phys. Chem. Chem. Phys.*, 2005, **7**, 3297–3305.
- 59 E. C. Tyo, M. Nossler, R. Mitric, V. Bonacic-Koutecky and A. W. Castleman, *Phys. Chem. Chem. Phys.*, 2011, **13**, 4243–4249.
- 60 E. Janssens, G. Santambrogio, M. Brümmer, L. Wöste, P. Lievens, J. Sauer, G. Meijer and K. R. Asmis, *Phys. Rev. Lett.*, 2006, **96**, 233401.
- 61 V. A. Rassolov, J. A. Pople, M. A. Ratner and T. L. Windus, *J. Chem. Phys.*, 1998, **109**, 1223–1229.
- 62 A. K. Rappe and E. R. Bernstein, *J. Phys. Chem. A*, 2000, **104**, 6117–6128.
- 63 S. F. Boys and F. Bernardi, *Mol. Phys.*, 2002, **100**, 65–73.
- 64 F. Bernardi, M. Olivucci and M. A. Robb, *Chem. Soc. Rev.*, 1996, **25**, 321–328.
- 65 N. Govind, K. Lopata, R. Rousseau, A. Andersen and K. Kowalski, *J. Phys. Chem. Lett.*, 2011, **2**, 2696–2701.
- 66 S. A. Chambers, S. H. Cheung, V. Shunthanandan, S. Thevuthasan, M. K. Bowman and A. G. Joly, *Chem. Phys.*, 2007, **339**, 27–35.
- 67 S. H. Cheung, P. Nachimuthu, A. G. Joly, M. H. Engelhard, M. K. Bowman and S. A. Chambers, *Surf. Sci.*, 2007, **601**, 1754–1762.
- 68 D. Schröder, S. Shaik and H. Schwarz, *Acc. Chem. Res.*, 2000, **33**, 139–145.